

Gradient Projection For Parameter-Efficient Continual Learning

Jingyang Qiao, Zhizhong Zhang, Xin Tan, Yanyun Qu, Wensheng Zhang, Yuan Xie, *Member, IEEE*,

Abstract—Catastrophic forgetting poses the primary challenge in the continual learning process of deep neural networks. Nowadays, methods based on parameter-efficient tuning (PET), which involves adding tiny extra parameters, have demonstrated impressive performance and promising perspectives in continual learning. However, these methods are still confronted with a common problem: fine-tuning on consecutive distinct tasks can disrupt the existing parameter distribution and lead to forgetting. Recent progress mainly focused in empirically designing efficient tuning engineering, lacking investigation of forgetting generation mechanism, anti-forgetting criteria and providing theoretical support. Additionally, the unresolved trade-off between learning new content and protecting old knowledge further complicates these challenges. The gradient projection methodology restricts gradient updates to the orthogonal direction of the old feature space, preventing distribution of the parameters from being damaged during updating and significantly suppressing forgetting. Developing on it, in this paper, we reformulate Adapter, LoRA, Prefix, and Prompt to continual learning setting from the perspective of gradient projection, and propose a unified framework called **Parameter Efficient Gradient Projection (PEGP)**. Based on the hypothesis that old tasks should have the same results after model updated, we introduce orthogonal gradient projection into different PET paradigms and theoretically demonstrate that the orthogonal condition for the gradient can effectively resist forgetting in PET-based continual methods. Notably, PEGP is the first unified method to provide an anti-forgetting mechanism with mathematical demonstration for different tuning paradigms. Additionally, through experiments on a novel cross-modality dataset BITM, we further discover that PEGP can not only alleviate forgetting but also suppress the appearance of hallucination during continual learning process, which provide a new insight for addressing hallucination in the cross-modality continual learning. We extensively evaluate our method with different backbones on diverse datasets, and experiments demonstrate its efficiency in reducing forgetting in class incremental, online class incremental, domain incremental, task incremental, and multi-modality incremental settings. The project page is available at <https://jingyangqiao.github.io/>.

Index Terms—continual learning, parameter-efficient tuning, anti-catastrophic forgetting, orthogonal gradient projection, multi-modality learning.



1 INTRODUCTION

DEEP neural networks are expected to learn continually while not forgetting as humans [1], [25], [35], [65]. Continual learning, or incremental learning is proposed to train a model with continuously expanded novel classes or domains in this context [7], [14], [45]. In general, continual learning includes four distinct settings, *i.e.*, task-, domain-, class- and online-incremental learning, abbreviated as TIL, DIL, CIL and OIL respectively [15], [51]. The main differences are (i). whether the task identifier, *i.e.*, the samples belong to which training tasks, is given for inference (TIL, CIL). (ii). whether the domain is changing in distinct tasks (DIL). (iii). whether the training samples can be seen only once (OIL).

However, the phenomenon that models exhibit a propensity to adapt to the knowledge of the current task while concurrently eroding the memory of preceding ones, *i.e.* catastrophic forgetting, deeply restricts the performance

of continual learning methods [12], [29], [36], [39]. In seeking to address the problem, many efforts have been proposed, including data rehearsal, parameter regularization, and model expansion [3], [6], [20], [23], [34], [44], [47], [54], [62]–[64]. However, these methods are prone to increase the risk of privacy leakage or memory burden and even lead to considerable forgetting when tasks become numerous.

Recently, the appearance of parameter-efficient tuning provides a new sight for continual learning [13], [33], [49], [58], [59]. In this framework, a tiny set of trainable parameters, *i.e.*, prompts or adapters are inserted into a fixed Transformer architecture. It indicates that these extra parameters not only can generalize the pre-trained knowledge to downstream tasks in sequence but also own well stability [10], [43]. However, as the parameter-efficient tuning originates from natural language processing (NLP), its deep anti-forgetting mechanism still remains unexplored [69].

Fortunately, gradient projection (GP) method indicates that continually learning would not forget if the gradient is updated in the orthogonal direction to the subspace spanned by the old features [11], [46], [55]. It modifies the gradient into an orthogonal direction by gradient projection matrix, which is obtained by extracting from sampled feature space. Furthermore, it can provide the anti-forgetting mechanism consuming with fewer extra memory space and training time. However, one obvious limitation is that the mathematical mechanism of GP is based on convolutional

- J. Qiao, Z. Zhang, X. Tan and Y. Xie are with School of Computer Science and Technology, East China Normal University, Shanghai, 200062, China; E-mail: {52275901010, zzzhang, xtan, yxie}@cs.ecnu.edu.cn
- W. Zhang is with Institute of Automation, Chinese Academy of Sciences, Beijing, 100190, China; E-mail: wensheng.zhang@ia.ac.cn
- Y. Qu is with School of Information Science and Technology, Xiamen University, Fujian, 361005, China; E-mail: yyqu@xmu.edu.cn

learned knowledge would cover old ones, leading to forgetting. Hereby, the S-Prompts method has been proposed by utilizing task-specific prompts which were only trainable in the corresponding task and frozen in other tasks [57]. However, assigning an independent prompt to each task would bring a memory burden as the task number increasing and task identifier inference is also an unsolved challenge. To reduce forgetting while only introducing fewer new prompts in each task, based on Prefix-tuning, DualPrompt divided the prompts into two parts: expert prompt (task-specific) and general prompt (task-shared) for distinct features learning and inserted them into different layers [59].

Although PET-based continual learning methods show state-of-the-art performance, forgetting still exists. Due to the limited connection between distinct PETs, previous works mainly focus on researching few of them [49], [58], [59]. One unified parameter-efficient continual method considers about four tuning paradigms (Prompt-tuning, Prefix-tuning, Adapter and LoRA) by a simple and direct EMA method to resist forgetting [13]. However forgetting is not explicitly modeled in this framework, its mechanism against forgetting has not been revealed yet.

In contrast to the above literature, our work is the first to theoretically demonstrate how to suppress catastrophic forgetting in PET-based continual learning. Besides that, we propose a unified framework to solve the forgetting problem in the four tuning paradigms mentioned above. Its effectiveness is verified in Sec.5.

2.3 Background of Gradient Projection Method

Gradient limitation, *i.e.*, restricting the gradient direction, originated from exquisite mathematical theory, provides an important explanation of the stability-plasticity dilemma [4], [32], [67].

Recent studies found that learning would not forget if the gradient is updated in the orthogonal direction to the subspace [60] spanned by the old features. Gradient projection method (GPM) updated the weights in the direction orthogonal to the subspace spanned by all previously learned inputs [46]. This ensured that new learning processes did not interfere with previously learned tasks. Trust Region Gradient Projection (TRGP) selected old tasks in the trust region to learn new tasks by a layer-wise scaling matrix, together with orthogonal gradient projection [30]. Simple Linear Connector (Connector) merged two models by using a weighted sum function where one model is updated normally and another is updated with gradient projection [31].

To further illustrate the anti-forgetting reason of gradient projection, we denote the inputs of task t for layer l as S_t^l , the learned model for task t as $\{W_t^l\}_{l=1}^L$, and L is the total number of layers. In the subsequent sections, we omit layer L for simplicity. Let ΔW_t denote the model change after learning task $t + 1$. If the update direction is orthogonal to the old features, it follows that $\Delta W_t x_{t,i} = 0$, and $x_{t,i} \in S_t$, where the index " t, i " means the i -th input image of task t . Therefore, the model W_{t+1} is updated as $W_{t+1} = W_t + \Delta W_t$. When validating the performance of model W_{t+1} on task t ,

we have:

$$W_{t+1}x_{t,i} = (W_t + \Delta W_t)x_{t,i} = W_t x_{t,i} + \Delta W_t x_{t,i} = W_t x_{t,i}, \quad (1)$$

which indicates that no interference is introduced to old tasks after learning a new concept, thereby addressing the forgetting issue.

However, one limitation of gradient projection methods is which is only applicable to convolutional neural networks but lack theory foundation in parameter efficient tuning based on vision-transformer. In this paper, we will prove that gradient projection methods can be an aid in resisting forgetting for parameter efficient tuning and the combination of these two methods shows advanced properties in continual learning with experiments.

2.4 Differences From the Preliminary Version

This study is a journal extension of the conference paper with the following differences and improvements [41]:

(1) The motivations differ- our prior work [41] only focuses on addressing the forgetting problem in Prompt/Prefix-based continual learning. However, PEGP proposes a unified framework that can simultaneously solve the problem in total four parameter-efficient tuning paradigms.

(2) The formulations are different. Our prior work provides a specific deduction and solution to alleviate forgetting in Prompt/Prefix-tuning. PEGP instead supplementally resolves the forgetting existing in Adapter/LoRA, and migrates from single modality model, ViT, to cross-modality models, CLIP.

(3) The prerequisites are looser. In our prior work, we extra introduce key-query mechanism with providing task-identifier, which can be aid of updating proper prompts with projected gradient. While in this work, we discover that gradient projection method can also work well without task identifier.

(4) We newly construct a cross-modality continual learning dataset called BITM, which can further validate the ability of continual learning methods with the task of image-text matching. We implement the baseline methods and the proposed PEGP framework on it. Experiments show that compared with baselines, PEGP can obviously improve the performance.

(5) We extensively evaluate PEGP across diverse continual learning scenes and provide comprehensive ablations isolating each key component. The substantial performance gain across all scenes verifies both the theoretical soundness and practical effectiveness of our modeling choice.

3 PRELIMINARY

In this section, we first provide a brief review of the self-attention mechanism in vision-transformer [9]. Then we introduce several variations of propositions depicting the mathematical, or idea conditions of anti-forgetting, which are also the final aims of our method. We summarize the basic notations and their descriptions in Table 1.

3.1 Self-Attention Mechanism

The self-attention mechanism enables the Transformer to capture relations across all the elements of the sequence [9]. Initially, with projection matrices W_q , W_k and W_v , the Query, Key, and Value are computed from the input sequence x of length l : $Q = W_q x$, $K = W_k x$, $V = W_v x$, where $W_q, W_k, W_v \in \mathcal{R}^{d_k \times l}$. Then, the attention matrix is calculated as:

$$\text{Attention}(Q, K, V) = \text{softmax}\left(\frac{QK^T}{\sqrt{d_k}}\right)V, \quad (2)$$

where d_k represents the projected dimension of the Query and Key. The attention formula obtained from a scaled dot-product between queries and keys: closer queries and key vectors will yield higher dot products (higher attention score). After that, the softmax function ensures that the attention weights range between 0 and 1 [2]. Finally, the attention matrix will be multiplied with the Value.

Here, to prevent the dot products leading gradient explosion in the backward propagation, the dot products are scaled by $\sqrt{d_k}$.

3.2 Parameter Efficient Tuning Paradigms

Parameter-efficient tuning only trains the extra added parameters while keeping the backbones frozen. Here, we mainly introduce four main-stream parameter-efficient tuning methods.

Adapter [18]: Extra trainable modules (adapters) are prepended into distinct transformer layers. The adapter generally uses a down-sampling layer with weights $W_{down} \in \mathcal{R}^{d \times r}$ to reduce dimension from a higher dimension d to a lower dimension r , followed by a nonlinear activation function $f(\cdot)$, and an up-sampling layer with weights $W_{up} \in \mathcal{R}^{r \times d}$ to restore dimension from r to d , which can be written as:

$$h = W_0 x + W_{up} f(W_{down} x). \quad (3)$$

LoRA [19]: LoRA prepends tiny trainable low-rank matrices into distinct transformer layers to substitute the update of backbone parameters: $W + \Delta W = W + W_{up} W_{down}$. Similar as Adapter, LoRA owns a low-rank down-sampling matrix with $W_{down} \in \mathcal{R}^{d \times r}$ and a low-rank up-sampling matrix with $W_{up} \in \mathcal{R}^{r \times d}$ as tunable parameters. For a specific input x , LoRA modifies the output as:

$$h = W_0 x + s W_{up} W_{down} x, \quad (4)$$

where s is a scalar control hyperparameter.

Prefix-Tuning [27]: A tiny set of parameters: prefix vectors $p \in \mathcal{R}^{L_p \times D}$, with sequence length L_p and embedding dimension D , are prepended to the keys and values at distinct layers to assist in predicting. In a multi-head self-attention (MSA) layer, the prompt is split into two parts $[p_K, p_V] \in \mathcal{R}^{\frac{L_p}{2} \times D}$ and contacted with key K and value V in this layer as $[p_K; K]$ and $[p_V; V]$ respectively. Thus, the final output of this layer can be seen as:

$$O(p, h) = \text{MSA}(p_Q, [p_K; K], [p_V; V]). \quad (5)$$

Prompt-Tuning [26]: As the simplified version of prefix tuning, Prompt-tuning only prepends one tunable prompt

vector $P \in \mathcal{R}^{l \times d}$ before the first transformer block. It is designed to be concatenated with the input word embeddings in the first layer. Then the concatenated vector is projected as query Q , key K , and value V . The computation of multi-head attention is calculated as:

$$\text{head}_1 = \text{Attn}(W_q^1 z, W_k^1 z, W_v^1 z). \quad (6)$$

Here, we have $z = \text{concat}(P, x)$.

4 METHOD

The proposed PEGP reformulates the traditional gradient projection into the PET (including Prompt, Prefix, Adapter, LoRA) based setting, and further derives their sufficient conditions towards anti-forgetting. In each subsection, we start from the proposition for individual PET method and deduce the equations which can address the catastrophic forgetting (Sec 4.1, 4.2, 4.3). Additionally, we also provide the solution based on the gradient projection method about how to realize the equations. Fortunately, we have found that these anti-forgetting equations own an union formation. Basis on these facts, we intuitively propose an unified framework of parameter-efficient continual tuning (Sec 4.4). Our motivations and the proposed methods are shown in Figure 2. Finally, we discuss the distinctions and improvements between the proposed PEGP method with other works and our previous work [41] in the discussion part of each subsection. To verify the cross-modality continual learning ability of our method, we specially build a novel image-text matching dataset based on the CUB200 dataset in Sec 4.5.

TABLE 1: Basic notations and their meaning descriptions.

| Notation | Meaning |
|--------------------------|--|
| $f_\theta(\cdot)$ | backbone network |
| $f_{act}(\cdot)$ | activation layer function |
| x_t^i, x_{t+1}^i | input of the first (i -th) layer at the t -th task |
| p_t^i, p_{t+1}^i | prompt of the first layer at the t -th ($t+1$ -th) task |
| p_t^{ik}, p_{t+1}^{ik} | prefix that inserts in the key of the i -th layer at the t -th ($t+1$ -th) task |
| p_t^{iv}, p_{t+1}^{iv} | prefix that inserts in the value of the i -th layer at the t -th ($t+1$ -th) task |
| W_q^i | Projection matrix of query corresponding to the i -th model layer |
| W_k^i | Projection matrix of key corresponding to the i -th model layer |
| W_v^i | Projection matrix of value corresponding to the i -th model layer |
| W_t^{di}, W_{t+1}^{di} | Down-dimension matrix of the i -th layer at the t -th ($t+1$ -th) task |
| W_t^{ui}, W_{t+1}^{ui} | Up-dimension matrix of the i -th layer at the t -th ($t+1$ -th) task |
| s | scalar hyperparameter |

Hypothesis 1 (zero-forgetting ideal condition). *The old inputs from previous tasks have the same outputs with parameters trained at old task and parameters after learning a new task.*

4.1 Prompt-based Gradient Projection Method

Considering the first layer of the backbone network, inputs x^1 and outputs h^1 of this layer can be described as:

$$h^1 = f_\theta^1(p^1, x^1). \quad (7)$$

To better preserve old knowledge, the update of network would satisfy the following propositions:

Proposition 1. *Starting from the old inputs from previous tasks x_t^1 have the same outputs after learning a new task, we have:*

$$f_\theta^1(p_{t+1}^1, x_t^1) = f_\theta^1(p_t^1, x_t^1). \quad (8)$$

In order to realize Proposition 1, we start from the implementation of Prompt-based continual learning (PCL).

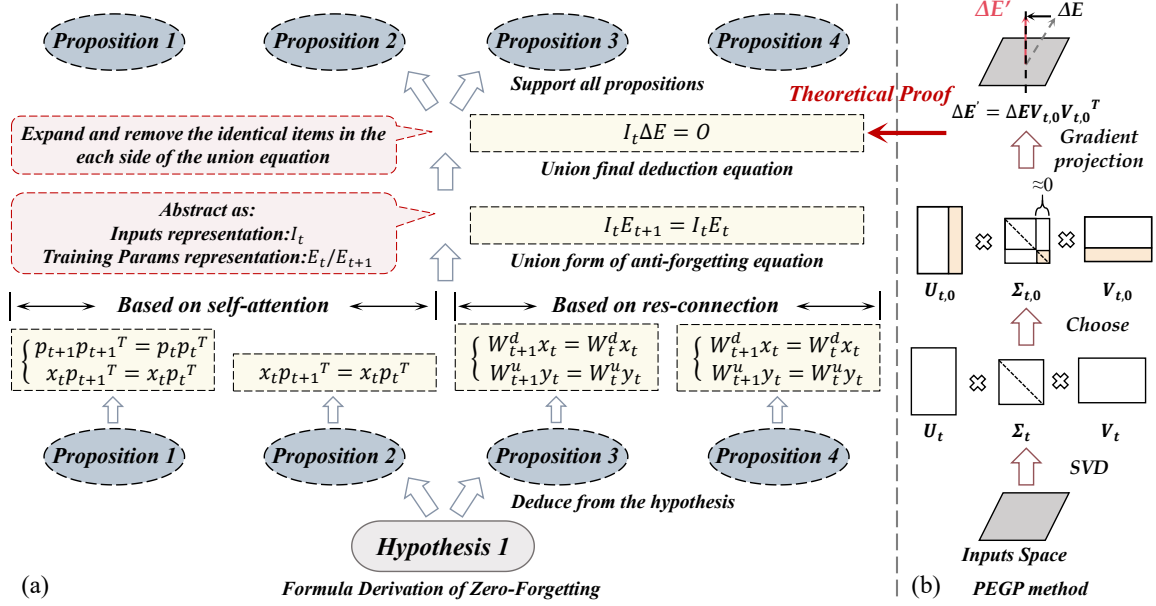


Fig. 2: Illustration of our motivations and methods. (a) An uniform anti-forgetting formula deduction process of four PETs, starting from the Hypothesis 1. (b) Our proposed PEGP method implementation process, including feature space sampling, singular vector decomposition, gradient projection matrix obtaining and gradient projection.

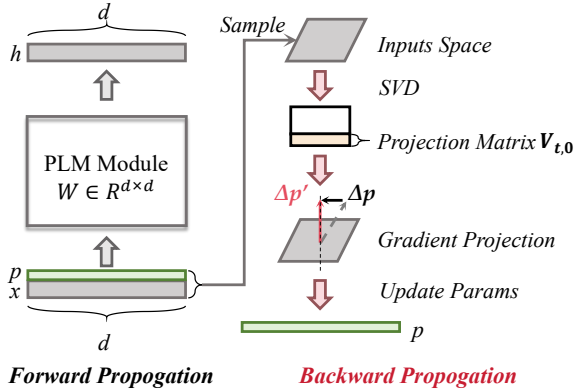


Fig. 3: Flowchart for Prompt-based continual learning.

In this framework, after the training of task $t + 1$, we concatenate the prompts p_{t+1} and the embedding sequences x_t , i.e., inputs from t -th task, along the embedding dimension: $Z_t^{t+1} = \begin{bmatrix} p_{t+1} \\ x_t \end{bmatrix}$. With the weights of W_q , W_k , W_v , PCL adopts the transformer architecture that allows us to obtain query ($Q_t^{t+1} = W_q Z_t^{t+1}$) and key ($K_t^{t+1} = W_k Z_t^{t+1}$). Thus the attention matrix [9] is calculated as:

$$A_t^{t+1} = \text{softmax}\left(\frac{Q_t^{t+1} K_t^{t+1 T}}{\sqrt{\left(\frac{d}{h}\right)}}\right). \quad (9)$$

Here, the denominator denotes a normalized factor and hence our focus turns to the numerator part $Q_t^{t+1} K_t^{t+1 T}$. It actually can be further expanded as $W_q Z_t^{t+1} Z_t^{t+1 T} W_k^T$. Notice that W_q and W_k , the weights of visual encoder, are frozen and unchanged during training. The parameters influenced by training are Z_t^{t+1} , $Z_t^{t+1 T}$. Similarly, with the old embedding Z_t^t , which is obtained through the concatenating

prompts trained at task t and embedding sequences x_t , we have $Z_t^t \cdot Z_t^{t T}$.

To realize Proposition 1, i.e., the condition of anti-forgetting, we need to achieve $Z_t^{t+1} \cdot Z_t^{t+1 T} = Z_t^t \cdot Z_t^{t T}$. Thus, the new prompts require to be:

$$\begin{cases} p_{t+1} p_{t+1}^T = p_t p_t^T, \\ x_t p_{t+1}^T = x_t p_t^T, \\ p_{t+1} x_t^T = p_t x_t^T. \end{cases} \quad (10)$$

For the rigours mathematical demonstrating process please kindly refer to A.1 in the supplementary materials for more details.

In Eq.(10), we divide p_{t+1} into p_t and Δp , where Δp is the gradient of prompts when training task $t + 1$ ¹. Therefore, for the first term, we extend $p_{t+1} p_{t+1}^T$ as:

$$p_{t+1} p_{t+1}^T = (p_t + \Delta p)(p_t + \Delta p)^T \quad (11)$$

$$= p_t p_t^T + p_t \Delta p^T + \Delta p p_t^T + \Delta p \Delta p^T. \quad (12)$$

Here we ignore the high-order infinitesimal term of $\Delta p \Delta p^T$. Thus if $p_t \Delta p^T = 0$, the condition, i.e., $p_{t+1} p_{t+1}^T = p_t p_t^T$ can be realized. In the same way, the second condition can be transformed to:

$$x_t p_{t+1}^T = x_t (p_t^T + \Delta p^T) = x_t p_t^T + x_t \Delta p^T = x_t p_t^T. \quad (13)$$

Eliminating $x_t p_t^T$ on both sides, we have $x_t \Delta p^T = 0$. Note that this condition also satisfies the third term in Eq.(10) because $x_t p_{t+1}^T$ is the transpose of $p_{t+1} x_t^T$.

Therefore, our key observation is reached: restricting the gradient of prompts by the following equations can realize anti-forgetting:

$$\begin{cases} x_t \Delta p^T = 0, \\ p_t \Delta p^T = 0. \end{cases} \quad (14)$$

1. Here we omit the factor of learning rating since this simplification wouldn't influence our conclusion.

To solve this equation, we decompose x_t with SVD: $x_t = U_t \Sigma_t V_t^T$. Here, U_t and V_t contain singular vectors corresponding to singular values in Σ_t , and diagonal matrix Σ_t can be further divided as:

$$\Sigma_t = \begin{bmatrix} \Sigma_{t,1} & O \\ O & \Sigma_{t,0} \end{bmatrix}, \quad (15)$$

where $\Sigma_{t,1}$ denotes the non-zero elements of Σ_t (non-zero singular values) and $\Sigma_{t,0}$ denotes the near-zero elements of Σ_t [8]. Correspondingly, V_t can be divided into two parts along the column dimension: $V_t = [V_{t,1}, V_{t,0}]$. Thus, we have:

$$x_t[V_{t,1}, V_{t,0}] = U_t \begin{bmatrix} \Sigma_{t,1} & O \\ O & \Sigma_{t,0} \end{bmatrix}. \quad (16)$$

As a result, we obtain the following equation:

$$x_t V_{t,0} = U_t \begin{bmatrix} O \\ \Sigma_{t,0} \end{bmatrix} \approx O. \quad (17)$$

Let $\Delta p = \Delta p V_{t,0} V_{t,0}^T$, we can get:

$$x_t \Delta p^T = x_t (\Delta p V_{t,0} V_{t,0}^T)^T = x_t V_{t,0} V_{t,0}^T \Delta p^T = O. \quad (18)$$

Eq.(18) allows us to successfully meet the first requirement in Eq.(14), by taking $V_{t,0}$ as the gradient projection matrix. We also have a similar conclusion for the second requirement in Eq.(14).

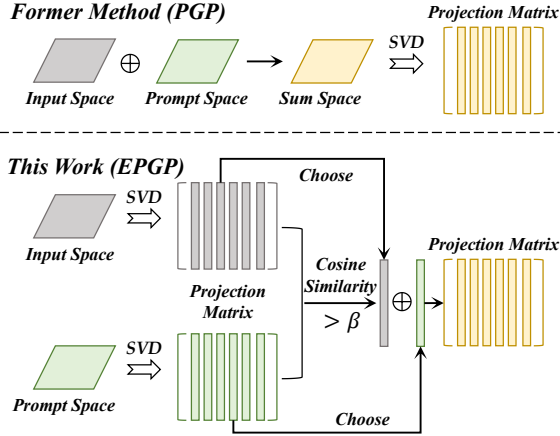


Fig. 4: Comparison of gradient projection matrix obtaining method between our previous work and this work.

In our previous work, we sum the prompt space and inputs space directly to create the sum space [41]. Based on the sum space, we calculate the gradient projection matrix. However, following with our further research, we find that the summation strategy would fail if the column vectors from each space own totally different directions, influencing the result of gradient projection. In this paper, we propose a novel gradient projection construction method. Here we calculate the cosine similarity between the column vectors of $V_{t,0}$ and $V_{t,0}^p$, where $V_{t,0}$ denotes the projection matrix of inputs and $V_{t,0}^p$ refers to the projection matrix of prompt. Then we compare the similarity score with a hyperparameter threshold β . If the score is larger which means that the two column vectors have similar directions, we sum the two column vectors and put the result into the final projection matrix $V_{t,0}$. Otherwise, we continue to compare the residual column vectors. The whole process is shown in Figure 4.

Discussion: Compared with other Prompt-based continual learning [49], [58], Eq.(10) not only reveals the mechanism of forgetting generation, but also provides three significant conditions to resist forgetting. On the other hand, it is essentially to propose a novel gradient projection calculation method to replace the summation method, as summation would break the direction of the feature space.

4.2 Prefix-based Gradient Projection Method

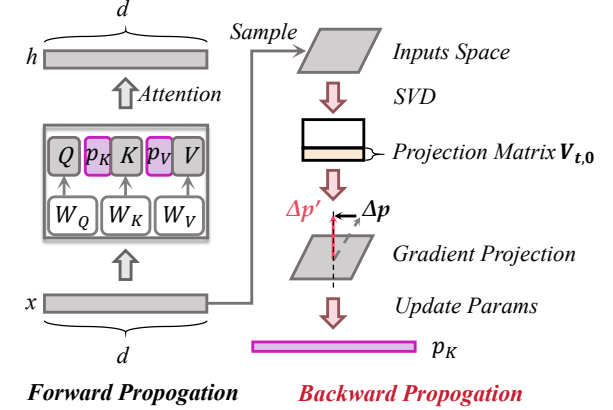


Fig. 5: Flowchart for Prefix-based continual learning.

Considering a layer with Prefix-Tuning module, inputs x^i and outputs h^i of this layer can be described as:

$$h^i = f_{\theta}^i(W_q^i x^i, W_k^i[p^{ik}, x^i], W_v^i[p^{iv}, x^i]). \quad (19)$$

To better preserve old knowledge, the update of network would satisfy the following propositions:

Proposition 2. Starting from the old inputs from previous tasks x_t^i have the same outputs after learning a new task, we have:

$$f_{\theta}^i(W_q^i x_t^i, W_k^i z_t^{ik}, W_v^i z_t^{iv}) = f_{\theta}^i(W_q^i x_t^i, W_k^i z_{t+1}^{ik}, W_v^i z_{t+1}^{iv}). \quad (20)$$

In the subsequent sections, we omit layer i for simplicity. Assuming that a set of prefixes have been trained at task $t + 1$, we input samples from task t and results can be represent as h_{t+1} with the prefixes on task $t + 1$, h_t with the prefixes on task t . Based on this notation, we have $h_t = A_t V_t$ and $h_{t+1} = A_{t+1} V_{t+1}$, where A_t and A_{t+1} refers to the corresponding attention matrix. With Proposition 2, we need to achieve $h_t = h_{t+1}$. By observing, we have the following solution:

$$\begin{cases} A_t = A_{t+1}, \\ V_t = V_{t+1}. \end{cases} \quad (21)$$

Now, we prepend prefixes on task $t + 1$ in the key/value vector and have:

$$Q_t = W_q x_t, \quad (22)$$

$$K_t = \begin{bmatrix} p_{t+1}^k \\ W_k x_t \end{bmatrix}, \quad (23)$$

$$V_t = \begin{bmatrix} p_{t+1}^v \\ W_v x_t \end{bmatrix}. \quad (24)$$

For the second equation in Eq.(21), due to the frozen weight W_v , the unique solution is $p_t^v = p_{t+1}^v$, which means

that the prefix of value equals to zero or not update. 1) Without prepended prefix maybe influence the ability adapted to the downstream task, further reduce the performance. 2) Although frozen prefix could satisfy the equation well, it would stop learning new knowledge leading to degradation of new task accuracy. Thus, we might not have a perfect solution for this condition, and the forgetting here are avoidable.

However for the first equation in Eq.(21), where W_q and W_k are weights, frozen and unchanged. With Eq.(9), we have the equation that satisfy the first equation in Eq.(21) as:

$$x_t p_{t+1}^T = x_t p_t^T, \quad (25)$$

which has the same form as Eq.(13), meaning that we can also achieve Eq.(25) by the gradient projection method. Thus, we can draw the conclusion that the gradient projection method could also help models based on prefix-tuning to resist forgetting. For the rigours mathematical demonstrating process please kindly refer to A.2 in the supplementary materials for more details.

Discussion: Compared with other Prefix-based continual learning [49], [59], Eq.(25) not only reveals the mechanism of forgetting generation, but also provides one significant condition to resist forgetting. On the other hand, compared with our previous work [41], in this paper, we additionally discuss about the influence of the update of prefix prepended in the value vector. Although it could generate forgetting phenomena, there is no excellent addressing method existing.

4.3 Adapter/LoRA-based Gradient Projection Method

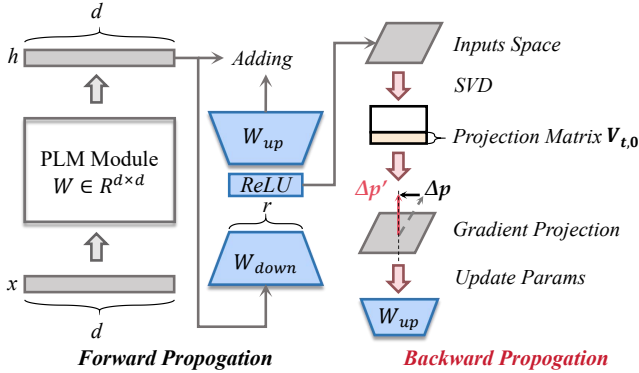


Fig. 6: Flowchart for Adapter-based continual learning.

Considering a layer with Adapter module, inputs x^i and outputs h^i of this layer can be described as:

$$h^i = f_{\theta}^i(x^i) + f_{act}(W^{ui}W^{di}x^i). \quad (26)$$

Proposition 3. Starting from the old inputs from previous tasks x_t^i have the same outputs after learning a new task, we have:

$$f_{\theta}^i(x_t^i) + f_{act}(W_t^{ui}W_t^{di}x_t^i) = f_{\theta}^i(x_t^i) + f_{act}(W_{t+1}^{ui}W_{t+1}^{di}x_t^i). \quad (27)$$

Considering a layer with LoRA module, inputs x^i and outputs h^i of this layer can be described as:

$$h^i = f_{\theta}^i(x^i) + s \cdot W^{ui}W^{di}x^i. \quad (28)$$

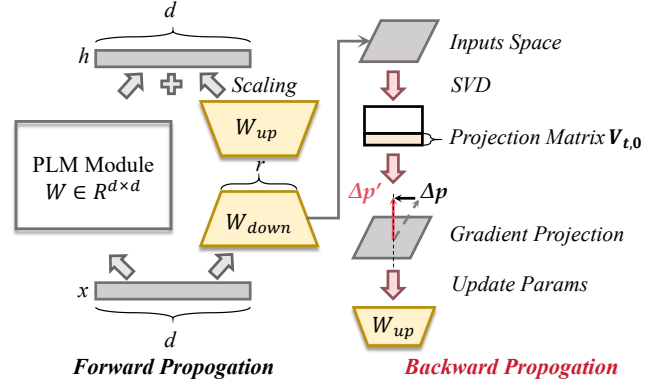


Fig. 7: Flowchart for LoRA-based continual learning.

Proposition 4. Starting from the old inputs from previous tasks x_t^i have the same outputs after learning a new task, we have:

$$f_{\theta}^i(x_t^i) + s \cdot W_t^{ui}W_t^{di}x_t^i = f_{\theta}^i(x_t^i) + s \cdot W_{t+1}^{ui}W_{t+1}^{di}x_t^i. \quad (29)$$

From Proposition 3 and Proposition 4, if we eliminate identical terms on both sides of these two equations respectively, we have:

$$\begin{cases} f_{act}(W_t^{ui}W_t^{di}x_t^i) = f_{act}(W_{t+1}^{ui}W_{t+1}^{di}x_t^i), \\ s \cdot W_t^{ui}W_t^{di}x_t^i = s \cdot W_{t+1}^{ui}W_{t+1}^{di}x_t^i. \end{cases} \quad (30)$$

Based on the above equation, if we omit the scalar hyperparameter s and activation layer function f_{act} , we can find that the mathematical form of Adapter is highly similar to LoRA. Thus, we can discuss the two tuning paradigms about resisting forgetting together. Through observing the Eq.(30), we can both obtain the following equation:

$$W_t^{ui}W_t^{di}x_t^i = W_{t+1}^{ui}W_{t+1}^{di}x_t^i. \quad (31)$$

Define the update of W^{di} , W^{ui} as ΔW^{di} and ΔW^{ui} . We can present the W_{t+1}^{di} and W_{t+1}^{ui} by W_t^{di} and W_t^{ui} as:

$$\begin{cases} W_{t+1}^{di} = W_t^{di} + \Delta W^{di}, \\ W_{t+1}^{ui} = W_t^{ui} + \Delta W^{ui}. \end{cases} \quad (32)$$

By substituting Eq.(32) into Eq.(31), we can obtain:

$$W_t^{ui}W_t^{di}x_t^i = (W_t^{di} + \Delta W^{di})(W_t^{ui} + \Delta W^{ui})x_t^i. \quad (33)$$

By comparing the two ends of the equations, it can be observed that the above equation can be derived from:

$$\begin{cases} W_{t+1}^{di}x_t^i = (W_t^{di} + \Delta W^{di})x_t^i, \\ W_{t+1}^{ui}y_t^i = (W_t^{ui} + \Delta W^{ui})y_t^i, \end{cases} \quad (34)$$

where $y_t^i = W_t^{di}x_t^i = W_{t+1}^{di}x_t^i$, removing the identical items in the both sides of Eq.(34) yields:

$$\begin{cases} \Delta W^{di}x_t^i = 0, \\ \Delta W^{ui}y_t^i = 0. \end{cases} \quad (35)$$

Therefore, our goal shifts from achieving Proposition 3 and Proposition 4 to Eq.(35). Observing Eq.(35), it can be seen that the two equations have the same form. Therefore, their implementation methods should also be identical.

To achieve Eq.(35), we perform singular value decomposition and obtain $SVD(x_t^i) = U_t^i \Sigma_t^i V_t^{iT}$. Further we have

$U_t^{iT} x_t^i = \Sigma_t^i V_t^{iT}$. By selecting only the eigenvectors in U_t^i corresponding to zero or close to zero eigenvalues, we can obtain:

$$U_{t,0}^{iT} x_t^i = \Sigma_{t,0}^i V_{t,0}^{iT} = \begin{bmatrix} O \\ \Sigma_{t,0}^i \end{bmatrix} V_{t,0}^{iT} \approx O. \quad (36)$$

Thus, if we choose $U_{t,0}^i U_{t,0}^{iT}$ as the projection matrix, then we have: $\Delta W^{di} = \Delta W^{di} U_{t,0}^i U_{t,0}^{iT}$. At this point, it holds that:

$$\Delta W^{di} x_t^i = \Delta W^{di} U_{t,0}^i U_{t,0}^{iT} x_t^i = 0. \quad (37)$$

Similarly, we can also achieve $\Delta W^{ui} y_t^i = 0$. Therefore, we can ultimately achieve Proposition 3 and Proposition 4.

Discussion: Compared with other Adapter/LoRA-based continual learning [13], [68], Eq.(34) not only reveals the mechanism of forgetting generation, but also provides two significant conditions to resist forgetting. On the other hand, compared with our previous work [41], we expand the application scopes of gradient projection method from Prompt/Prefix-based continual learning to Adapter/LoRA-based. We not only present the theoretical demonstration, but also detailed implementation method.

4.4 An Unified Parameter-Efficient Continual Method

Considering the general case with all parameter tuning paradigms, we discover that they own the similar anti-forgetting equations and can be described by an union equation. Prima facie, assuming that the old inputs are denoted as I_t and the new/old trainable parameters as E_{t+1} , E_t respectively, we can have the following equation to abstract generalize:

$$I_t E_{t+1} = I_t E_t. \quad (38)$$

Expand E_{t+1} as $E_{t+1} = E_t + \Delta E$ and remove the identical items in the each side of the union equation. Finally, we can obtain:

$$I_t \Delta E = 0. \quad (39)$$

In the proposed PEGP method, to realize Eq.(39), firstly, we sample the feature space of inputs I_t . Then we utilize the singular value decomposition method to extract the gradient projection column vectors according to the near-zero singular value. Here for the updating of gradient projection matrix, we follow the GPM method [46]. In each task, we continually add the column vectors which are unique and orthogonal to the existing column vectors in gradient projection matrix. In this way, we can not only update the gradient projection matrix well, but also prevent the memory explosion. After that, we project on the gradient with the gradient projection matrix as $\Delta E' = \Delta E V_{t,0} V_{t,0}^T$. Finally, we use modified gradient $\Delta E'$ to update the parameter E .

Discussion: Compare with previous works, we firstly unify the anti-forgetting mechanism and propose a union anti-forgetting method. Notice that, although they have distinct starting point, e.g. Prompt/Prefix from self-attention mechanism, Adapter/LoRA from residual connection, their anti-forgetting mechanism can be described jointly. It shows that our method is independent from the specific tuning mechanism and own strong generalization ability, which

means that the proposed method have huge undiscovered potential and can be applied in more tuning paradigms in the future.

4.5 Cross-modality Incremental Learning Task

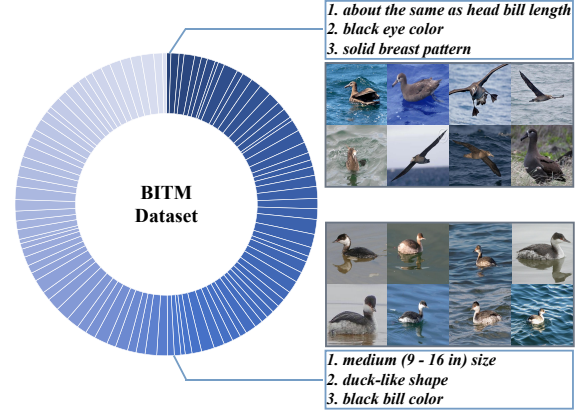


Fig. 8: Visualization of BITM: a novel text-image matching dataset. In the figure, each sector represents a class, and the size of the sector represents the number of images in the corresponding class. The larger the sector, the more images in the corresponding class

In order to further validate the effectiveness of our method in cross-modality incremental learning task, we constructed a novel text-image matching dataset based on the CUB200 dataset [53]. The specific construction method is as follows:

First of all, we select the first 100 classes from the CUB200 dataset. Based on attribute annotations, we extract attributes with certainties of 4 (definitely) and 3 (probably) of each class. These attributes are then sorted based on their frequency of occurrence in images, and the top three attributes with the highest frequency are selected as the text labels. Next, we select images which simultaneously possessed these text labels from the image set. These selected images, along with the text labels, form the text-image matching dataset. We name this new dataset as BITM (Bird Image Text Matching Dataset) and analyze the distribution of text labels and images in the dataset. The visualization of the dataset is shown in the Figure 8. The statistics reveal that BITM contains 100 bird species with a total of 3714 images. The class with the highest number of images contains 59 images, while the class with the lowest number of images contains 13 images. On average, each class contains about 35 images. We divide the dataset into training and testing sets in the ratio of 8:2. Considering that BITM is a continual learning dataset, we further split the dataset into 10-Split-BITM and 5-Split-BITM, where each task contains 10 and 20 classes of images, respectively.

5 EXPERIMENTS

In this section, we show the proposed PEGP framework could be flexibly applied to various continual learning tasks: (i) Class/Online class Incremental Learning; (ii) Domain Incremental Learning; (iii) Task Incremental Learning; (iv)

TABLE 2: Class incremental learning (*i.e.*, task identifier is unknown at test phase) results of Avg. ACC and Forgetting on 10-Split-CIFAR100 and 10-Split-ImageNet-R with ViT backbone.

| Method | Avenue | Paradigm | 10-Split-CIFAR100 | | 10-Split-ImageNet-R | |
|-----------------|---------|------------|-------------------------|-----------------------------|-------------------------|-----------------------------|
| | | | Avg. Acc (\uparrow) | Forgetting (\downarrow) | Avg. Acc (\uparrow) | Forgetting (\downarrow) |
| Baseline | - | Adapter-5 | 79.96 | 12.60 | 62.23 | 18.58 |
| | | Adapter-10 | 79.17 | 13.81 | 61.98 | 19.71 |
| | | LoRA-5 | 78.26 | 12.66 | 61.19 | 17.13 |
| | | LoRA-10 | 79.45 | 12.60 | 61.49 | 18.27 |
| | | Prompt-10 | 78.92 | 9.88 | 58.98 | 11.77 |
| | | Prompt-20 | 80.13 | 9.32 | 59.37 | 11.71 |
| | | Prefix-10 | 77.04 | 11.32 | 58.95 | 13.13 |
| | | Prefix-20 | 77.68 | 11.80 | 60.08 | 12.98 |
| L2P [58] | CVPR'22 | Prompt | 83.12 | 7.66 | 68.38 | 6.93 |
| DualPrompt [59] | ECCV'22 | Prefix | 84.59 | 5.60 | 68.57 | 6.29 |
| LAE [13] | ICCV'23 | Adapter-5 | 84.75 | 7.43 | 70.72 | 9.62 |
| | | Adapter-10 | 85.10 | 6.69 | 70.82 | 9.89 |
| | | LoRA-5 | 84.80 | 6.64 | 69.65 | 10.13 |
| | | LoRA-10 | 85.04 | 6.91 | 69.44 | 10.92 |
| | | Prompt-10 | 84.23 | 5.80 | 68.58 | 6.12 |
| | | Prompt-20 | 84.06 | 6.32 | 68.81 | 6.38 |
| | | Prefix-10 | 85.03 | 5.97 | 70.86 | 6.28 |
| | | Prefix-20 | 84.83 | 6.37 | 70.51 | 6.59 |
| PEGP | Ours | Adapter-5 | 85.16 | 6.09 | 71.59 | 5.62 |
| | | Adapter-10 | 85.43 | 6.38 | 71.70 | 5.85 |
| | | LoRA-5 | 85.02 | 6.54 | 70.30 | 6.35 |
| | | LoRA-10 | 85.14 | 6.23 | 70.54 | 6.04 |
| | | Prompt-10 | 84.69 | 5.47 | 69.30 | 5.94 |
| | | Prompt-20 | 84.46 | 6.11 | 69.31 | 6.10 |
| | | Prefix-10 | 85.35 | 5.75 | 71.04 | 6.09 |
| | | Prefix-20 | 85.30 | 6.11 | 70.79 | 6.27 |

Cross-modality Incremental Learning with distinct backbones (i) ViT; (ii) CLIP. The quantitative and qualitative results demonstrate the effectiveness of our approach in various circumstances. All experiments are held on NVIDIA RTX 4090 GPUs.

5.1 Evaluation Protocol

In this section, we introduce the adopted benchmark datasets and corresponding evaluation standards. We follow the most popular protocol for evaluation, where are average accuracy (Simplified as accuracy or Avg. Acc), forgetting, and new task accuracy (Simplified as New Acc) (please refer to B in the supplementary materials for more details).

5.2 Implementation Details

For ViT backbone. Consistent with previous works, we use ViT-B/16 pre-trained on ImageNet-21K as our image encoder [9], which is kept frozen during training. We adopt LAE model, which is a continual learning method contained Adapter/LoRA/Prefix/Prompt tuning paradigms, as our baseline, with removing the original online/offline dual model design and EMA model fusion mechanism. Instead, we add the proposed parameter efficient gradient projection method at the training stage to suppress forgetting.

For CLIP backbone. We utilize the model from our previous work [41], and the backbone is ViT-B-16 pre-trained by OpenAI [42]. On the vision side, we only set a single trainable image Prompt/Linear Adapter shared by all tasks. As for the text side, we set trainable text prompt for each class, which is only trained at the corresponding task according to CoOP [70]. Besides that, we add gradient projection

method at the training stage for efficient parameter and improve our gradient projection method by following [31], which linearly merges two models with/without gradient projection method [38].

5.3 Class/Online class/Task Incremental Learning

We first evaluate our approach on class incremental learning. In this setting, images usually come in a sequence of tasks. In each task, it usually contains the same number of classes, and the classes will not repeat or overlap. As task identifier would not be provided in the inference stage, the key challenge of this task hence lies in the mixture and covering of novel and previous knowledge, leading to catastrophic forgetting. To verify the effectiveness of PEGP framework, we also validate our method on a more challenging task, online class incremental learning, which only allows training data appearing once for protecting the user privacy [48]. Task incremental learning maintains the similar training mode with class incremental learning, while the only distinct is that task incremental learning allows for obtaining the task identifier at the inference stage. Therefore, it can be regarded as a weakened form of class incremental learning.

5.3.1 Benchmarks

10-Split-CIFAR100 [24] contains 20 major categories and 100 subcategories. For each subcategory, it owns 600 images (500 training images and 100 test images). We construct it by evenly splitting the 100 classes into 10 disjoint tasks, and each task has 10 classes.

10-Split-ImageNet-R [17] is deemed to mimic real-world scenarios with different image styles and intra-class diversity. It contains art, cartoons, deviantart, et al. 16 renditions of ImageNet classes. ImageNet-R has 200 ImageNet classes with total of 30,000 images. We split the total 200 classes into 10 disjoint tasks, and each task has 20 classes.

10-Split-ImageNet100 [40] is a sub-dataset of ImageNet Large scale Visual Recognition Challenge (ILSVRC), which selects 100 categories from ImageNet1K. The training set contains 600 annotated images for each class in total of 60000 images, and the validation set contains 100 annotated images for each class in total of 10000 images. We split the total 100 classes into 10 disjoint tasks, and each task has 10 classes.

5.3.2 Training Settings

For ViT backbone. We train the 10-Split-CIFAR100 for 5 epochs and 10-Split-ImageNet-R for 50 epochs with 24 images (resized as $224 \times 224 \times 3$) in each batch. Adapter/LoRA width is set at 5/10, and Prefix/Prompt length is set at 10/20 both for the two datasets. The initial learning rate is 0.0028125 for 10-Split-CIFAR100 and 0.00046875 for 10-Split-ImageNet-R, and the decay rate is 0 with Adam optimizer [2], [5], [22].

For CLIP backbone. We train the 10-Split-CIFAR100/10-Split-ImageNet100 for 5 epochs with 32 images (resized as $224 \times 224 \times 3$) in each batch. Linear Adapter width/Prompt length is set at 10 both for the two datasets. The initial learning rate is 0.001 for the first task and 0.01 for sequential tasks, while the decay rate is 0.1 with Adam optimizer.

TABLE 3: Online class incremental learning results of Avg. ACC and Forgetting on 10-Split-CIFAR100 dataset with ViT backbone.

| Method | Avenue | Paradigm | 10-Split-CIFAR100 | |
|-------------|---------|------------------|-------------------------|-----------------------------|
| | | | Avg. Acc (\uparrow) | Forgetting (\downarrow) |
| Baseline | - | Adapter-5 | 75.19 | 19.61 |
| Baseline | - | LoRA-5 | 76.58 | 16.00 |
| LAE [13] | ICCV'23 | Adapter-5 | 81.11 | 11.44 |
| LAE [13] | ICCV'23 | LoRA-5 | 78.30 | 12.17 |
| Ours | - | Adapter-5 | 83.77 | 6.82 |
| Ours | - | LoRA-5 | 83.21 | 7.47 |

5.3.3 Experimental Results

Comparison with ViT backbone. We compare the performance of our PEGP method with other SOTA methods in Table 2 under class incremental setting. We observe that PEGP can greatly improve the average accuracy and reduce the forgetting compared with baseline on the four tuning paradigms, demonstrating its effectiveness and generalization ability. It is also noteworthy that with the aid of gradient projection, PEGP outperforms other SOTA methods both on the two datasets by +0.33@Avg. ACC on the 10-Split-CIFAR100 benchmark and +0.88@Avg. ACC on the 10-Split-ImageNet-R benchmark.

The same experimental phenomena can also be explored under online class incremental learning in Table 3. Although the training process only allows one epoch for each task, our method still performs stronger anti-forgetting ability compared with baseline and others. Figure 9 and Figure 10

shows the curves of accuracy and forgetting with the task number increasing on 10-Split-CIFAR100. We observe that on all tasks, accuracy of our method is always higher than baseline, and forgetting is always lower than baseline with two different tuning paradigms.

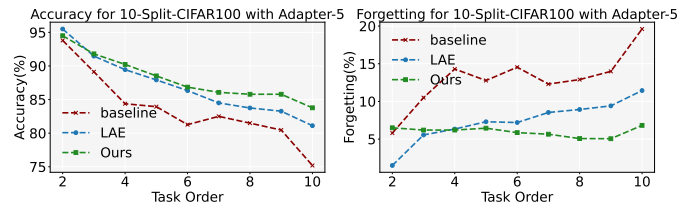


Fig. 9: Task-by-task performance changing curves in terms of accuracy and forgetting under online class incremental learning on 10-Split-CIFAR100 with Adapter-5.

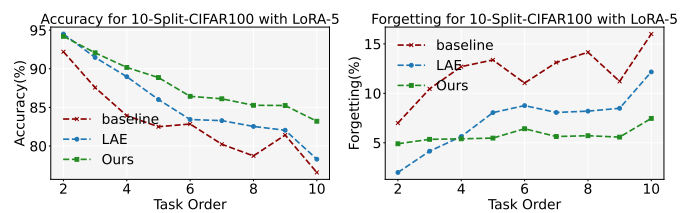


Fig. 10: Task-by-task performance changing curves in terms of accuracy and forgetting under online class incremental learning on 10-Split-CIFAR100 with LoRA-5.

Comparison with CLIP backbone. As we compare our method with other SOTA methods based on CLIP backbone, we see that the PEGP can also greatly bring decent improvements both on average accuracy and forgetting. Specifically, on 10-Split-CIFAR100, the method sees an improvement of +0.96 in average accuracy compared with SOTA method. Similarly, on 10-Split-ImageNet100, the method sees an improvement of surprisingly +1.40 in average accuracy compared with SOTA method. This validates that the introduction of gradient projection method with parameter efficient tuning improves model performance without requiring any additional learnable parameters.

While for task incremental setting, experiments show that our method owns the lowest forgetting but slightly lower accuracy than state-of-the-art on both two datasets in Table 5. Reasons we speculate is that plasticity and stability are trade-off in continual learning. If we focus more on maintaining stability, plasticity is inevitably affected, resulting in a decrease in overall average accuracy. To prove our above hypothesis, we present the new class accuracy changing curve for each of the 10 tasks, as shown in the Figure 11. It can be seen that the overall new task accuracy curve of our method is always lower than the SOTA method.

5.3.4 Ablation Study

Based on the Figure 12, we can draw the similar conclusions in Adapter/LoRA tuning case: With the change of hyper-parameter ϵ , leading to the prompt projection matrix $V_{t,0}$ with distinct numbers of column vectors. If the ϵ becomes smaller, more column vectors would be added into the $V_{t,0}$, causing lower new task accuracy (worse plasticity)

TABLE 4: Class incremental learning results on 10-Split-CIFAR100 and 10-Split-ImageNet100 dataset with CLIP backbone.

| Method | Avenue | Paradigm | 10-Split-CIFAR100 | | 10-Split-ImageNet100 | |
|---------------------|-------------|----------------|-------------------------|-----------------------------|-------------------------|-----------------------------|
| | | | Avg. Acc (\uparrow) | Forgetting (\downarrow) | Avg. Acc (\uparrow) | Forgetting (\downarrow) |
| Continual-CLIP [50] | ArXiv'22 | Prompt | 66.70 | - | 75.40 | - |
| CoOP(Baseline) [70] | IJCV'22 | Prompt | 73.76 | 5.60 | 83.66 | 2.47 |
| CoOP(Baseline) [70] | IJCV'22 | Adapter | 63.95 | 6.28 | 78.24 | 5.04 |
| CLIP-EWC [23] | PNAS'17 | Prompt | 72.29 | 6.31 | 81.92 | 3.58 |
| CLIP-LWF [28] | TPAMI'16 | Prompt | 75.44 | 7.42 | 84.10 | 2.38 |
| CLIP-PGP [41] | ICLR'24 | Prompt | 79.47 | 4.23 | 84.14 | 2.11 |
| AttriCLIP [56] | CVPR'23 | Prompt | 81.40 | - | 83.30 | - |
| CLIP-PEGP | Ours | Prompt | 82.36 (+8.60) | 2.82 (-2.78) | 85.54 (+1.88) | 1.80 (-0.67) |
| CLIP-PEGP | Ours | Adapter | 70.37 (+6.42) | 5.72 (-0.56) | 79.16 (+0.92) | 2.60 (-2.44) |

TABLE 5: Task incremental learning results on 10-Split-CIFAR100 and 10-Split-ImageNet100 dataset with CLIP backbone.

| Method | Avenue | Paradigm | 10-Split-CIFAR100 | | 10-Split-ImageNet100 | |
|---------------------|-------------|---------------|-------------------------|-----------------------------|-------------------------|-----------------------------|
| | | | Avg. Acc (\uparrow) | Forgetting (\downarrow) | Avg. Acc (\uparrow) | Forgetting (\downarrow) |
| CoOP(Baseline) [70] | IJCV'22 | Prompt | 92.69 | 2.34 | 89.08 | 1.98 |
| CLIP-EWC [23] | PNAS'17 | Prompt | 94.42 | 1.22 | 89.08 | 1.60 |
| CLIP-LWF [28] | TPAMI'16 | Prompt | 93.96 | 1.38 | 89.36 | 1.56 |
| CLIP-PGP [41] | ICLR'24 | Prompt | 93.00 | 1.58 | 88.75 | 1.73 |
| CLIP-PEGP | Ours | Prompt | 93.99 | 0.80 | 89.08 | 1.56 |

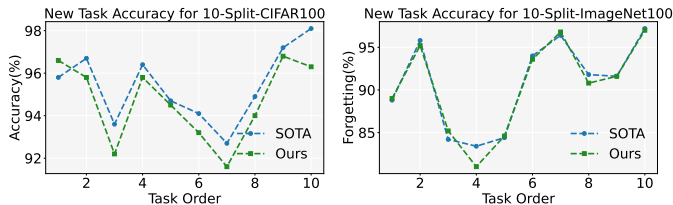


Fig. 11: Task-by-task performance changing curves in terms of new task accuracy with CLIP backbone under task incremental setting.

but less forgetting (better stability). On the contrary, bigger ϵ refers to the less column vectors in the $V_{t,0}$, resulting in more forgetting (worse stability) but higher new task accuracy (better plasticity).

Although here we only show the results with Adapter/LoRA tuning paradigms, similar phenomena are also observed in our previous work with Prompt/Prefix tuning paradigms and detailed mathematical mechanism behind them is also included [41]. Thus, We can recognize that the essence of the gradient projection method is a kind of trade-off strategy between plasticity and stability. However, different from other dilemmas [37], it has an optimal solution, which is projecting gradient in the direction orthogonal to the subspace spanned by the old inputs, which can not only own the best ability of anti-forgetting, but also have minimal damage to plasticity.

5.3.5 Visualization

To better visualize the improvement of our method, we also plot the 2D projection of representations, obtained from the visual output of CLIP, by using t-SNE on Figure 13 and Figure 14, where we compare the representations obtained

from our approach and baseline. The representations are from task 1 processed by model trained in task 9. By observing the scatters, we have: (i) the embedding space produced by baseline seems to be lack of discrimination, where we can spot obvious overlapping within some classes and indistinguishable boundaries between different categories; (ii) the gap distance between some classes of the embedding space produced by baseline looks like few or no. However, the above two problems have been well addressed in our method, suggesting the better continual learning ability and preserved old knowledge.

5.4 Domain Incremental Learning

Domain incremental learning aims to verify the continual domain adaption ability of methods. In this setting, images in each task come from distinct domains and the number and kinds of classes in each task should keep same. This scenario is therefore satisfactory to valid the anti-forgetting effectiveness of our PEGP method with changing domains.

5.4.1 Benchmarks

6-Split-DomainNet is a dataset for domain adaption and domain incremental learning, which has 345 categories and roughly 600,000 images. Images from DomainNet is split into 6 domains. Here, we deem the each domain as a task and each task has 345 classes.

5.4.2 Training Settings

We only adopt ViT backbone in this setting, and train the 6-Split-DomainNet for 50 epochs with 24 images (resized as 224*224*3) in each batch. Adapter/LoRA width is set at 5/10, and Prefix/Prompt length is set at 10/20. The initial learning rate is 0.00046875, and the decay rate is 0 with Adam optimizer.

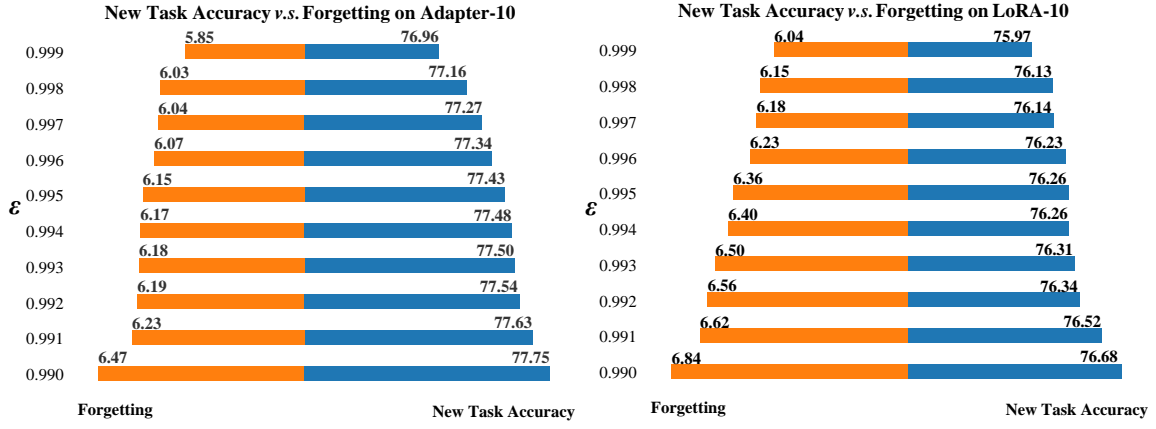


Fig. 12: Ablation study with threshold ϵ with Adapter-10/LoRA-10 paradigm on 10-Split-ImageNet-R.

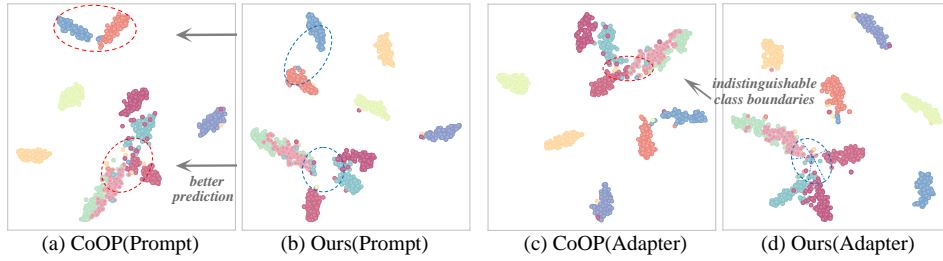


Fig. 13: t-SNE visualization of class incremental learning results on 10-Split-CIFAR100 based on CLIP backbone.

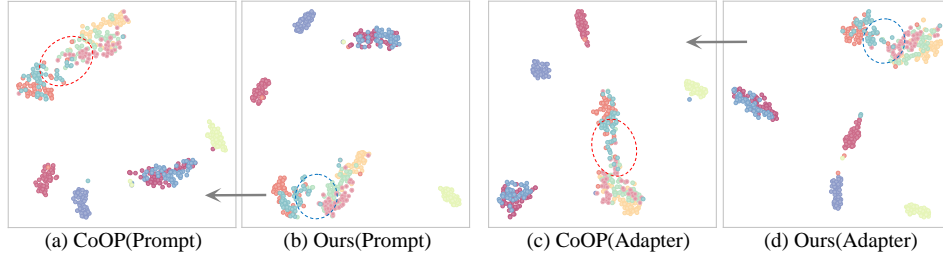


Fig. 14: t-SNE visualization of class incremental learning results on 10-Split-ImageNet100 based on CLIP backbone.

5.4.3 Experimental Results

Table 6 shows the comparison results of our PEGP method with baseline and LAE. We observe from the Table 6 that PEGP again sets a new state-of-the-art in this setting too. Compared to 6-Split-DomainNet where our method improves SOTA by +1.20@Avg. ACC and -3.54@Forgetting on the Adapter-10 paradigm at the most with the aid of gradient projection, demonstrating its excellent anti-forgetting and generalization ability for the four PET methods.

5.5 Cross-modality Incremental Learning

Cross-modality incremental learning intends to evaluate the multi-modality model in continually learning across modalities involved image and text. In this paper, we propose a novel image-text matching dataset called BITM, and verify the cross-modality continual learning capability of PEGP on it.

5.5.1 Benchmarks

5-Split-BITB/10-Split-BITB are two benchmarks for cross-modality continual learning, which have 100 fine-grained bird categories and 3714 images. Images from BITB is split into 5/10 disjoint tasks with 20/10 classes in each task.

5.5.2 Training Settings

We only adopt CLIP backbone in this setting, with utilizing the CoOP method and incorporating two different tuning paradigms, Prompt and Linear Adapter, into the image encoder as baselines. Additionally, in our method, we integrate PEGP into both Prompt and Linear Adapter. We train the 5-Split-BITB/10-Split-BITB for 30 epochs with 32 images (resized as 224*224*3) in each batch. Linear Adapter width/Prompt length is set at 10 both for the two datasets. The initial learning rate is 0.001 for the first task and 0.01 for sequential tasks, while the decay rate is 0.1 with Adam optimizer.

TABLE 6: Domain incremental learning results of Avg. ACC and Forgetting on DomainNet dataset with ViT backbone.

| Method | Width | Baseline | | LAE [13] | | Ours | |
|---------|-------|--------------|----------------|--------------|----------------|--------------|----------------|
| | | Avg. Acc (↑) | Forgetting (↓) | Avg. Acc (↑) | Forgetting (↓) | Avg. Acc (↑) | Forgetting (↓) |
| Adapter | 5 | 61.56 | 14.68 | 65.65 | 9.73 | 66.30 | 6.57 |
| | 10 | 61.40 | 16.23 | 65.85 | 10.38 | 67.05 | 6.84 |
| LoRA | 5 | 61.59 | 14.92 | 66.13 | 9.68 | 67.12 | 5.88 |
| | 10 | 61.80 | 15.51 | 66.09 | 10.77 | 67.17 | 6.46 |
| Prefix | 10 | 61.56 | 14.68 | 65.87 | 8.36 | 66.03 | 7.64 |
| | 20 | 61.46 | 13.99 | 65.80 | 8.95 | 66.25 | 8.13 |
| Prompt | 10 | 61.34 | 11.99 | 64.74 | 7.28 | 64.89 | 5.98 |
| | 20 | 61.41 | 12.28 | 64.82 | 7.43 | 65.23 | 6.38 |

TABLE 7: Cross-modality incremental learning results with CLIP backbone on BITM dataset.

| Method | Avenue | Paradigm | 10-Split-BITM | | 5-Split-BITM | |
|---------------------|-------------|---------------|---------------|----------------|--------------|----------------|
| | | | Avg. Acc (↑) | Forgetting (↓) | Avg. Acc (↑) | Forgetting (↓) |
| CoOP(Baseline) [70] | IJCV'22 | Prompt | 42.01 | 33.04 | 52.73 | 29.32 |
| CLIP-EWC [23] | PNAS'17 | Prompt | 50.20 | 32.62 | 37.03 | 25.82 |
| CLIP-LWF [28] | TPAMI'16 | Prompt | 55.81 | 23.48 | 18.31 | 49.07 |
| CLIP-PEGP | Ours | Prompt | 55.70 | 22.97 | 62.66 | 23.38 |

5.5.3 Experimental Results

We compare the performance of our PEGP method with baseline and other SOTA methods in Table 7. We observe that PEGP can greatly improve the average accuracy and reduce the forgetting compared with baseline on the two benchmarks with distinct tuning paradigms, demonstrating its effectiveness and generalization ability. It is also noteworthy that with the aid of gradient projection, PEGP can not only reduce the forgetting, but also alleviate the hallucination appearing in the training process. In Figure 15, we can clearly observe that hallucination present during continually sequential fine-tuning. [66] deem that the hallucination problem in large models is related to the forgetting problem in continual learning, and it can be grouped as external hallucination and internal hallucination. The above view is consistent with our experimental results. However, when comparing with our method, we are surprised to find that PEGP can spontaneously suppress the occurrence of hallucination. We believe that this is inseparable from the anti-forgetting ability of our method. Therefore, we propose that mitigating illusions in large models can be examined through the perspective of reducing forgetting. This discovery may pave the way for addressing the issue of hallucination in large models.

6 CONCLUSION

In this work, we theoretically demonstrate that the orthogonal gradient projection can effectively resist forgetting and be applicable to all PET-based continual learning methods. On this basis, we provide a unified framework, Parameter Efficient Gradient Projection, to address the catastrophic forgetting for different tuning paradigms. Additionally, PEGP is proven to be the optimal solution for balancing the trade-off between plasticity and stability in PET-based continual learning methods by choosing the gradient projection matrix. Surprisingly, we also discover that the proposed method aids in overcoming the hallucination problem in the




| Input image | GT | Baseline | Ours |
|--|---|--|---|
|  | black eye color all-purpose bill shape yellow underparts color | black eye color yellow underparts color yellow breast color | black eye color all-purpose bill shape yellow underparts color |
|  | the same as head bill length black eye color spatulate bill shape | the same as head bill length plain head pattern hooked seabird bill shape | the same as head bill length black eye color spatulate bill shape |
|  | the same as head bill length black eye color spatulate bill shape | shorter than head bill length black primary color solid back pattern | the same as head bill length black eye color black bill color |

Fig. 15: Examples of cross-modality incremental learning results. The red marked attributes represent the hallucinations in baseline, while the blue marked attributes represent the predictions corresponding to our method.

continual learning process. The future works would include learning on the large language or multi modality model to further verify the potential of gradient projection method. Also, more broader learning applications such as image generation or segmentation would be studied.

APPENDIX

A. PROOF DETAILS

A.1 Proof to Anti-forgetting Equations in Prompt-tuning

In Prompt-tuning paradigm, to realize the Proposition 1, we have the following result from $Z_t^{t+1} \cdot Z_t^{t+1}$:

$$Z_t^{t+1} \cdot Z_t^{t+1T} = \begin{bmatrix} p_{t+1} \\ x_t \end{bmatrix} \begin{bmatrix} p_{t+1}^T & x_t^T \end{bmatrix} = \begin{bmatrix} p_{t+1}p_{t+1}^T & p_{t+1}x_t^T \\ x_t p_{t+1}^T & x_t x_t^T \end{bmatrix}. \quad (40)$$

By contrast, the old embedding Z_t^t , is obtained through the concatenating prompts trained at task t and embedding sequences x_t :

$$Z_t^t \cdot Z_t^{tT} = \begin{bmatrix} p_t \\ x_t \end{bmatrix} \begin{bmatrix} p_t^T & x_t^T \end{bmatrix} = \begin{bmatrix} p_t p_t^T & p_t x_t^T \\ x_t p_t^T & x_t x_t^T \end{bmatrix}. \quad (41)$$

To achieve Proposition 1, *i.e.*, the condition of anti-forgetting, the new prompts require to be:

$$\begin{cases} p_{t+1}p_{t+1}^T = p_t p_t^T, \\ x_t p_{t+1}^T = x_t p_t^T, \\ p_{t+1}x_t^T = p_t x_t^T. \end{cases} \quad (42)$$

A.2 Proof to Anti-forgetting Equations in Prefix-tuning

Assuming that a set of prefixes have been trained at task $t+1$, we input samples from task t . Now, we prepend prefix in the key vector and have:

$$Q_t^{t+1} = W_q x_t, \quad (43)$$

$$K_t^{t+1} = \begin{bmatrix} p_{t+1} \\ W_k x_t \end{bmatrix}, \quad (44)$$

where, W_q and W_k are weights of i -th layer, frozen and unchanged. With Eq.(9), we have the results that t -th task samples on $t+1$ -th model. We mainly focus on the part:

$$\begin{aligned} Q_t^{t+1} K_t^{t+1T} &= W_q x_t [p_{t+1}^T \quad (W_k x_t)^T] \\ &= [W_q x_t p_{t+1}^T \quad W_q x_t x_t^T W_k^T]. \end{aligned}$$

As stable item $W_q x_t x_t^T W_k^T$, we only focus on the item $W_q x_t p_{t+1}^T$. Changing p_{t+1}^T with p_t^T , we can obtain the results that t -th task samples on t -th model:

$$\begin{aligned} Q_t^t K_t^{tT} &= W_q x_t [p_t^T \quad (W_k x_t)^T] \\ &= [W_q x_t p_t^T \quad W_q x_t x_t^T W_k^T]. \end{aligned}$$

Because our aim is making $W_q x_t p_{t+1}^T$ equal to $W_q x_t p_t^T$, considering that W_q is frozen, our final aim can be simplified as:

$$x_t p_{t+1}^T = x_t p_t^T, \quad (45)$$

B. EVALUATION METRICS

Three metrics: Average Accuracy (Avg. ACC), Forgetting (FOR), and New Task Accuracy (New. ACC) are used to evaluate the performance. We use average accuracy metric, for average test classification accuracy of all tasks. We adopt forgetting metric to indicate the loss of accuracy of past tasks after learning the last new task. We employ new task accuracy metric, for average test classification accuracy of new tasks.

$$\text{Average Accuracy} = \frac{1}{T} \sum_{i=1}^T A_{T,i}, \quad (46)$$

$$\text{Forgetting} = \frac{1}{T-1} \sum_{i=1}^{T-1} A_{T,i} - \max(A_{j,i})_{j \in [i, T-1]}, \quad (47)$$

$$\text{New Task Accuracy} = \frac{1}{T} \sum_{i=1}^T A_{i,i}, \quad (48)$$

where T is the number of tasks, $A_{T,i}$ is the accuracy of i -th task samples on the T -th model, $A_{j,i}$ is the accuracy of i -th task samples on the j -th model, and $A_{i,i}$ is the accuracy of i -th task samples on the i -th model.

Algorithm 1: Training phase

Input: Pre-trained ViT model f_θ , classifier f_c ,
number of tasks T , training set
 $\{\{x_i^t, y_i^t\}_{i=1}^{n_t}\}_{t=1}^T$, sampling set
 $\{\{x_{si}^t, y_{si}^t\}_{i=1}^{n_{st}}\}_{t=1}^T$, efficient parameters p ,
number of training epochs E , projection
matrix $V_{t,0}$, cross-entropy loss \mathcal{L}_{CE} , learning
rate η

initialize: f_c, p
for $t = 1, \dots, T$ **do**
 for $e_1 = 1, \dots, E_1$ **do**
 1: Draw a mini-batch $B = \{\{x_i^t, y_i^t\}_{i=1}^{n_t}\}$
 for (x, y) **in** B **do**
 2: Obtain prediction by $\hat{y} = f_c(f_\theta(p, x))$
 3: Calculate sample loss $\mathcal{L}_x = \mathcal{L}_{CE}(y, \hat{y})$
 end
 4: Obtain batch loss \mathcal{L}_B by accumulating \mathcal{L}_x
 end
 # Parameter Efficient Gradient Projection
 if $t = 1$ **then**
 5. Update p by $p \leftarrow p - \eta \nabla_p \mathcal{L}_B$.
 else
 6. Update p by $p \leftarrow p - \eta \nabla_p \mathcal{L}_B V_{t,0} V_{t,0}^T$.
 end
 # Gradient Projection Matrix Update
 7. Initialize the sets of sampled features: $X_t = \{\}$.
 for (x, y) **in** $\{\{x_{si}^t, y_{si}^t\}_{i=1}^{n_{st}}\}$ **do**
 8. Sample set of features X_t from $f_\theta(p, x)$.
 9. Update $V_{t,0}$ by X_t .
 end
end

C. ALGORITHM

REFERENCES

- [1] E. Arani, F. Sarfraz, and B. Zonooz, "Learning fast, learning slow: A general continual learning method based on complementary learning system," *arXiv preprint arXiv:2201.12604*, 2022.
- [2] J. S. Bridle, "Probabilistic interpretation of feedforward classification network outputs, with relationships to statistical pattern recognition," in *Neurocomputing: Algorithms, architectures and applications*. Springer, 1990, pp. 227–236.
- [3] P. Buzzega, M. Boschini, A. Porrello, D. Abati, and S. Calderara, "Dark experience for general continual learning: a strong, simple baseline," *Advances in neural information processing systems*, vol. 33, pp. 15 920–15 930, 2020.
- [4] A. Chaudhry, N. Khan, P. Dokania, and P. Torr, "Continual learning in low-rank orthogonal subspaces," *Advances in Neural Information Processing Systems*, vol. 33, pp. 9900–9911, 2020.
- [5] P.-T. De Boer, D. P. Kroese, S. Mannor, and R. Y. Rubinstein, "A tutorial on the cross-entropy method," *Annals of operations research*, vol. 134, pp. 19–67, 2005.
- [6] A. Chaudhry, M. Ranzato, M. Rohrbach, and M. Elhoseiny, "Efficient lifelong learning with a-gem," *arXiv preprint arXiv:1812.00420*, 2018.
- [7] M. De Lange, R. Aljundi, M. Masana, S. Parisot, X. Jia, A. Leonardis, G. Slabaugh, and T. Tuytelaars, "A continual learning survey: Defying forgetting in classification tasks," *IEEE transactions on pattern analysis and machine intelligence*, vol. 44, no. 7, pp. 3366–3385, 2021.
- [8] M. P. Deisenroth, A. A. Faisal, and C. S. Ong, *Mathematics for machine learning*. Cambridge University Press, 2020.
- [9] A. Dosovitskiy, L. Beyer, A. Kolesnikov, D. Weissenborn, X. Zhai, T. Unterthiner, M. Dehghani, M. Minderer, G. Heigold, S. Gelly *et al.*, "An image is worth 16x16 words: Transformers for image recognition at scale," *arXiv preprint arXiv:2010.11929*, 2020.

- [10] A. Douillard, A. Ramé, G. Couairon, and M. Cord, "Dytox: Transformers for continual learning with dynamic token expansion," in *Proceedings of the IEEE/CVF Conference on Computer Vision and Pattern Recognition*, 2022, pp. 9285–9295.
- [11] M. Farajtabar, N. Azizan, A. Mott, and A. Li, "Orthogonal gradient descent for continual learning," in *International Conference on Artificial Intelligence and Statistics*. PMLR, 2020, pp. 3762–3773.
- [12] R. M. French, "Catastrophic forgetting in connectionist networks," *Trends in cognitive sciences*, vol. 3, no. 4, pp. 128–135, 1999.
- [13] Q. Gao, C. Zhao, Y. Sun, T. Xi, G. Zhang, B. Ghanem, and J. Zhang, "A unified continual learning framework with general parameter-efficient tuning," in *Proceedings of the IEEE/CVF International Conference on Computer Vision*, 2023, pp. 11 483–11 493.
- [14] R. Hadsell, D. Rao, A. A. Rusu, and R. Pascanu, "Embracing change: Continual learning in deep neural networks," *Trends in cognitive sciences*, vol. 24, no. 12, pp. 1028–1040, 2020.
- [15] J. He, R. Mao, Z. Shao, and F. Zhu, "Incremental learning in online scenario," in *Proceedings of the IEEE/CVF conference on computer vision and pattern recognition*, 2020, pp. 13 926–13 935.
- [16] K. He, X. Zhang, S. Ren, and J. Sun, "Deep residual learning for image recognition," in *Proceedings of the IEEE conference on computer vision and pattern recognition*, 2016, pp. 770–778.
- [17] D. Hendrycks, S. Basart, N. Mu, S. Kadavath, F. Wang, E. Dorundo, R. Desai, T. Zhu, S. Parajuli, M. Guo *et al.*, "The many faces of robustness: A critical analysis of out-of-distribution generalization," in *Proceedings of the IEEE/CVF International Conference on Computer Vision*, 2021, pp. 8340–8349.
- [18] N. Houlsby, A. Giurgiu, S. Jastrzebski, B. Morrone, Q. De Larousilhe, A. Gesmundo, M. Attariyan, and S. Gelly, "Parameter-efficient transfer learning for nlp," in *International conference on machine learning*. PMLR, 2019, pp. 2790–2799.
- [19] E. J. Hu, Y. Shen, P. Wallis, Z. Allen-Zhu, Y. Li, S. Wang, L. Wang, and W. Chen, "Lora: Low-rank adaptation of large language models," *arXiv preprint arXiv:2106.09685*, 2021.
- [20] D. Isele and A. Cosgun, "Selective experience replay for lifelong learning," in *Proceedings of the AAAI Conference on Artificial Intelligence*, vol. 32, no. 1, 2018.
- [21] M. G. Z. A. Khan, M. F. Naeem, L. Van Gool, D. Stricker, F. Tombari, and M. Z. Afzal, "Introducing language guidance in prompt-based continual learning," *arXiv preprint arXiv:2308.15827*, 2023.
- [22] D. P. Kingma and J. Ba, "Adam: A method for stochastic optimization," *arXiv preprint arXiv:1412.6980*, 2014.
- [23] J. Kirkpatrick, R. Pascanu, N. Rabinowitz, J. Veness, G. Desjardins, A. A. Rusu, K. Milan, J. Quan, T. Ramalho, A. Grabska-Barwinska *et al.*, "Overcoming catastrophic forgetting in neural networks," *Proceedings of the national academy of sciences*, vol. 114, no. 13, pp. 3521–3526, 2017.
- [24] A. Krizhevsky, G. Hinton *et al.*, "Learning multiple layers of features from tiny images," 2009.
- [25] D. Kumaran, D. Hassabis, and J. L. McClelland, "What learning systems do intelligent agents need? complementary learning systems theory updated," *Trends in cognitive sciences*, vol. 20, no. 7, pp. 512–534, 2016.
- [26] B. Lester, R. Al-Rfou, and N. Constant, "The power of scale for parameter-efficient prompt tuning," *arXiv preprint arXiv:2104.08691*, 2021.
- [27] X. L. Li and P. Liang, "Prefix-tuning: Optimizing continuous prompts for generation," *arXiv preprint arXiv:2101.00190*, 2021.
- [28] Z. Li and D. Hoiem, "Learning without forgetting," *IEEE transactions on pattern analysis and machine intelligence*, vol. 40, no. 12, pp. 2935–2947, 2017.
- [29] X. Li, Y. Zhou, T. Wu, R. Socher, and C. Xiong, "Learn to grow: A continual structure learning framework for overcoming catastrophic forgetting," in *International conference on machine learning*. PMLR, 2019, pp. 3925–3934.
- [30] S. Lin, L. Yang, D. Fan, and J. Zhang, "Trgp: Trust region gradient projection for continual learning," *arXiv preprint arXiv:2202.02931*, 2022.
- [31] G. Lin, H. Chu, and H. Lai, "Towards better plasticity-stability trade-off in incremental learning: A simple linear connector," in *Proceedings of the IEEE/CVF Conference on Computer Vision and Pattern Recognition*, 2022, pp. 89–98.
- [32] D. Lopez-Paz and M. Ranzato, "Gradient episodic memory for continual learning," *Advances in neural information processing systems*, vol. 30, 2017.
- [33] Z. Ma, X. Hong, B. Liu, Y. Wang, P. Guo, and H. Li, "Remind of the past: Incremental learning with analogical prompts," *arXiv preprint arXiv:2303.13898*, 2023.
- [34] A. Mallya and S. Lazebnik, "Packnet: Adding multiple tasks to a single network by iterative pruning," in *Proceedings of the IEEE conference on Computer Vision and Pattern Recognition*, 2018, pp. 7765–7773.
- [35] J. L. McClelland, B. L. McNaughton, and R. C. O'Reilly, "Why there are complementary learning systems in the hippocampus and neocortex: insights from the successes and failures of connectionist models of learning and memory," *Psychological review*, vol. 102, no. 3, p. 419, 1995.
- [36] M. McCloskey and N. J. Cohen, "Catastrophic interference in connectionist networks: The sequential learning problem," in *Psychology of learning and motivation*. Elsevier, 1989, vol. 24, pp. 109–165.
- [37] M. Mermillod, A. Bugaiska, and P. Bonin, "The stability-plasticity dilemma: Investigating the continuum from catastrophic forgetting to age-limited learning effects," *Frontiers in psychology*, vol. 4, p. 54654, 2013.
- [38] S. I. Mirzadeh, M. Farajtabar, D. Gorur, R. Pascanu, and H. Ghahemzadeh, "Linear mode connectivity in multitask and continual learning," *arXiv preprint arXiv:2010.04495*, 2020.
- [39] C. V. Nguyen, A. Achille, M. Lam, T. Hassner, V. Mahadevan, and S. Soatto, "Toward understanding catastrophic forgetting in continual learning," *arXiv preprint arXiv:1908.01091*, 2019.
- [40] O. Russakovsky, J. Deng, H. Su, J. Krause, S. Satheesh, S. Ma, Z. Huang, A. Karpathy, A. Khosla, M. Bernstein, A. C. Berg, and L. Fei-Fei, "ImageNet Large Scale Visual Recognition Challenge," *International Journal of Computer Vision (IJCV)*, vol. 115, no. 3, pp. 211–252, 2015.
- [41] J. Qiao, Z. Zhang, X. Tan, C. Chen, Y. Qu, Y. Peng, and Y. Xie, "Prompt gradient projection for continual learning," in *The Twelfth International Conference on Learning Representations*, 2023.
- [42] A. Radford, J. W. Kim, C. Hallacy, A. Ramesh, G. Goh, S. Agarwal, G. Sastry, A. Askell, P. Mishkin, J. Clark *et al.*, "Learning transferable visual models from natural language supervision," in *International conference on machine learning*. PMLR, 2021, pp. 8748–8763.
- [43] A. Rannen, R. Aljundi, M. B. Blaschko, and T. Tuytelaars, "Encoder based lifelong learning," in *Proceedings of the IEEE international conference on computer vision*, 2017, pp. 1320–1328.
- [44] S.-A. Rebuffi, A. Kolesnikov, G. Sperl, and C. H. Lampert, "icarl: Incremental classifier and representation learning," in *Proceedings of the IEEE conference on Computer Vision and Pattern Recognition*, 2017, pp. 2001–2010.
- [45] M. B. Ring, "Child: A first step towards continual learning," *Machine Learning*, vol. 28, pp. 77–104, 1997.
- [46] G. Saha, I. Garg, and K. Roy, "Gradient projection memory for continual learning," *arXiv preprint arXiv:2103.09762*, 2021.
- [47] J. Serra, D. Suris, M. Miron, and A. Karatzoglou, "Overcoming catastrophic forgetting with hard attention to the task," in *International conference on machine learning*. PMLR, 2018, pp. 4548–4557.
- [48] R. Shokri and V. Shmatikov, "Privacy-preserving deep learning," in *Proceedings of the 22nd ACM SIGSAC conference on computer and communications security*, 2015, pp. 1310–1321.
- [49] J. S. Smith, L. Karlinsky, V. Gutta, P. Cascante-Bonilla, D. Kim, A. Arbelle, R. Panda, R. Feris, and Z. Kira, "Coda-prompt: Continual decomposed attention-based prompting for rehearsal-free continual learning," in *Proceedings of the IEEE/CVF Conference on Computer Vision and Pattern Recognition*, 2023, pp. 11 909–11 919.
- [50] V. Thengane, S. Khan, M. Hayat, and F. Khan, "Clip model is an efficient continual learner," *arXiv preprint arXiv:2210.03114*, 2022.
- [51] G. M. Van de Ven and A. S. Tolias, "Three scenarios for continual learning," *arXiv preprint arXiv:1904.07734*, 2019.
- [52] A. Vaswani, N. Shazeer, N. Parmar, J. Uszkoreit, L. Jones, A. N. Gomez, Ł. Kaiser, and I. Polosukhin, "Attention is all you need," *Advances in neural information processing systems*, vol. 30, 2017.
- [53] C. Wah, S. Branson, P. Welinder, P. Perona, and S. Belongie, "The caltech-ucsd birds-200-2011 dataset," 2011.
- [54] F.-Y. Wang, D.-W. Zhou, H.-J. Ye, and D.-C. Zhan, "Foster: Feature boosting and compression for class-incremental learning," in *European conference on computer vision*. Springer, 2022, pp. 398–414.
- [55] S. Wang, X. Li, J. Sun, and Z. Xu, "Training networks in null space of feature covariance for continual learning," in *Proceedings of the IEEE/CVF conference on Computer Vision and Pattern Recognition*, 2021, pp. 184–193.

- [56] R. Wang, X. Duan, G. Kang, J. Liu, S. Lin, S. Xu, J. Lü, and B. Zhang, "Attriclip: A non-incremental learner for incremental knowledge learning," in *Proceedings of the IEEE/CVF Conference on Computer Vision and Pattern Recognition*, 2023, pp. 3654–3663.
- [57] Y. Wang, Z. Huang, and X. Hong, "S-prompts learning with pre-trained transformers: An occam's razor for domain incremental learning," *Advances in Neural Information Processing Systems*, vol. 35, pp. 5682–5695, 2022.
- [58] Z. Wang, Z. Zhang, C.-Y. Lee, H. Zhang, R. Sun, X. Ren, G. Su, V. Perot, J. Dy, and T. Pfister, "Learning to prompt for continual learning," in *Proceedings of the IEEE/CVF Conference on Computer Vision and Pattern Recognition*, 2022, pp. 139–149.
- [59] Z. Wang, Z. Zhang, S. Ebrahimi, R. Sun, H. Zhang, C.-Y. Lee, X. Ren, G. Su, V. Perot, J. Dy *et al.*, "Dualprompt: Complementary prompting for rehearsal-free continual learning," in *European Conference on Computer Vision*. Springer, 2022, pp. 631–648.
- [60] M. Wortsman, M. C. Horton, C. Guestrin, A. Farhadi, and M. Rastegari, "Learning neural network subspaces," in *International Conference on Machine Learning*. PMLR, 2021, pp. 11 217–11 227.
- [61] Y. Wu, Y. Chen, L. Wang, Y. Ye, Z. Liu, Y. Guo, and Y. Fu, "Large scale incremental learning," in *Proceedings of the IEEE/CVF conference on computer vision and pattern recognition*, 2019, pp. 374–382.
- [62] S. Yan, J. Xie, and X. He, "Der: Dynamically expandable representation for class incremental learning," in *Proceedings of the IEEE/CVF conference on computer vision and pattern recognition*, 2021, pp. 3014–3023.
- [63] J. Yoon, E. Yang, J. Lee, and S. J. Hwang, "Lifelong learning with dynamically expandable networks," *arXiv preprint arXiv:1708.01547*, 2017.
- [64] G. Zeng, Y. Chen, B. Cui, and S. Yu, "Continual learning of context-dependent processing in neural networks," *Nature Machine Intelligence*, vol. 1, no. 8, pp. 364–372, 2019.
- [65] F. Zenke, B. Poole, and S. Ganguli, "Continual learning through synaptic intelligence," in *International conference on machine learning*. PMLR, 2017, pp. 3987–3995.
- [66] Y. Zhai, S. Tong, X. Li, M. Cai, Q. Qu, Y. J. Lee, and Y. Ma, "Investigating the catastrophic forgetting in multimodal large language models," *arXiv preprint arXiv:2309.10313*, 2023.
- [67] Z. Zhao, Z. Zhang, X. Tan, J. Liu, Y. Qu, Y. Xie, and L. Ma, "Rethinking gradient projection continual learning: Stability/plasticity feature space decoupling," in *Proceedings of the IEEE/CVF Conference on Computer Vision and Pattern Recognition*, 2023, pp. 3718–3727.
- [68] D.-W. Zhou, H.-J. Ye, D.-C. Zhan, and Z. Liu, "Revisiting class-incremental learning with pre-trained models: Generalizability and adaptivity are all you need," *arXiv preprint arXiv:2303.07338*, 2023.
- [69] D.-W. Zhou, Y. Zhang, J. Ning, H.-J. Ye, D.-C. Zhan, and Z. Liu, "Learning without forgetting for vision-language models," *arXiv preprint arXiv:2305.19270*, 2023.
- [70] K. Zhou, J. Yang, C. C. Loy, and Z. Liu, "Learning to prompt for vision-language models," *International Journal of Computer Vision*, vol. 130, no. 9, pp. 2337–2348, 2022.